Cureus
Part of SPRINGER NATURE

Open Access Case Report

Left Atrial Myxoma Mimicking Thrombus on Computed Tomography With Multiterritorial Systemic Embolization in an Elderly Woman: A Case Report

Sergio Rueda Góez [1], Mateo Zapata Naranjo [1], Tatiana Suárez Poveda [1], Miguel Roldán Pérez [2]

1. Radiology, Universidad de Antioquia, Medellín, COL 2. Pathology, Hospital Universitario de San Vicente Fundación, Medellín, COL

Corresponding author: Sergio Rueda Góez, sergio.ruedag@udea.edu.co

Review began 09/21/2026
Review ended 11/08/2026
Published 11/14/2026

© Copyright 2026
Rueda Góez et al. This is an open access article distributed under the terms of the Creative Commons Attribution License CC-BY 4.0., which permits unrestricted use, distribution, and reproduction in any medium, provided the original author and source are credited.

DOI: 10.7759/cureus.119666

Abstract

We report the case of an 86-year-old hypertensive woman who presented with syncope and, over a two-week hospital stay, developed embolic injury in five vascular beds: the brain, both kidneys, the spleen, the ileocolic mesenteric territory, and both lower limbs. Contrast-enhanced computed tomography (CT) showed a left atrial mass that was initially interpreted as thrombus, in the setting of electrocardiographically documented atrial fibrillation, left atrial enlargement, and renal and splenic infarcts. Transthoracic echocardiography subsequently characterized a mobile 50 × 32 mm mass suggestive of myxoma, and histopathologic examination of the resected mass and of the material retrieved at embolectomy confirmed cardiac myxoma. The patient died of septic shock secondary to anastomotic dehiscence and fecal peritonitis. In retrospect, the size, lobulated contour, unequivocal heterogeneous enhancement, and non-appendage location of the mass on CT favored myxoma over thrombus. We discuss these features, the multiterritorial pattern of embolic injury on brain magnetic resonance imaging (MRI) and CT angiography, and the limitations of retrospective interpretation. A left atrial filling defect accompanied by infarcts in multiple vascular beds warrants prompt echocardiographic evaluation and consideration of myxoma, even when the clinical context favors thrombus.

Categories: Radiology, Cardiology
Keywords: acute lower limb ischemia, cardiac myxoma, ischemic stroke, mesenteric ischemia, systemic embolism

Introduction

Primary cardiac tumors are rare, with a reported prevalence of 0.001% to 0.03% in autopsy series [1,2]. Cardiac myxoma has traditionally been regarded as the most common primary cardiac tumor in adults; since the 2021 World Health Organization classification recognized papillary fibroelastoma as the most frequent benign primary cardiac tumor, myxoma is ranked second among benign tumors in some series [1]. Myxomas arise most often in the left atrium, typically from the interatrial septum near the fossa ovalis, and predominate in women between the third and sixth decades of life [1,3]. Although most are sporadic, 5% to 10% occur within the Carney complex, an autosomal dominant syndrome linked to inactivating mutations of the PRKAR1A gene [1,4].

The clinical behavior of cardiac myxoma follows a well-recognized triad of intracavitary obstruction, constitutional symptoms, and systemic embolization [1,5]. Embolic events affect 20% to 45% of patients and frequently precede the diagnosis of the tumor [5,6]. The brain is the most common target, accounting for approximately half of embolic episodes, followed by the visceral arteries, the extremities, and the coronary arteries [6,7]. When embolization involves several vascular beds, the differential diagnosis includes infective endocarditis, atrial fibrillation with mural thrombus, and paradoxical embolism [5,8].

Echocardiography remains the first-line imaging tool for intracardiac masses, but computed tomography (CT) and magnetic resonance imaging (MRI) provide complementary information for tissue characterization and for differentiation from thrombus [9,10]. On CT, myxomas typically appear as spherical or ovoid, lobulated, hypoattenuating intracavitary masses with heterogeneous attenuation [11], and may show heterogeneous enhancement, whereas thrombi are usually avascular and non-enhancing [10]. Attenuation alone does not reliably separate the two entities, particularly on early arterial-phase acquisitions; size, site of origin, shape, mobility, and prolapse are more discriminating [9]. Acute ischemic lesions in several noncontiguous territories on brain MRI may also suggest a proximal embolic source [7,12].

We report an elderly woman in whom a left atrial mass was initially interpreted on CT as thrombus, in a context that reasonably favored this diagnosis, and who developed embolic injury in five vascular beds before histopathologic confirmation of myxoma. We describe which CT features, in retrospect, could have raised suspicion of myxoma, how multimodality imaging defined the embolic burden, and the practical lesson for radiologists when an intracardiac filling defect coexists with systemic infarcts.

How to cite this article
Rueda Góez S, Zapata Naranjo M, Suárez Poveda T, et al. (November 14, 2026) Left Atrial Myxoma Mimicking Thrombus on Computed Tomography With Multiterritorial Systemic Embolization in an Elderly Woman: A Case Report. Cureus 18(11): e119666. DOI 10.7759/cureus.119666

Case Presentation

An 86-year-old woman with a history of arterial hypertension and rheumatoid arthritis presented to the emergency department after a fall from standing height triggered by a syncopal episode. She reported dizziness and vomiting of food contents without abnormal movements, as well as five similar episodes over the preceding months. On physical examination, she was pale, hemodynamically stable, alert, and oriented, with no focal neurologic deficit. Pelvic and femoral radiographs ruled out fracture, and noncontrast head CT was normal.

An expanded history revealed a four-month constitutional syndrome with anorexia, asthenia, weight loss of approximately five kilograms over one month, hypogastric pain, and a self-limited episode of hematochezia. Upper gastrointestinal endoscopy demonstrated severe erosive peptic esophagitis, a type I hiatal hernia, and erythematous pangastritis. Shortly after the procedure, the patient had another episode of hematochezia and desaturation to 82%, requiring supplemental oxygen.

Contrast-enhanced CT of the chest (arterial phase) and abdomen (portal venous phase) was then obtained to investigate the unexplained constitutional symptoms and gastrointestinal bleeding. The study showed an oval intraluminal mass in the left atrium measuring 45 × 30 mm, with lobulated contours, heterogeneous enhancement, and no calcifications, in contact with the interatrial septum. It was interpreted at the time as an intracavitary thrombus. Wedge-shaped hypodense areas in both kidneys and the spleen were consistent with established infarcts (Figure *1*). Cardiomegaly with left atrial enlargement, diffuse calcified atherosclerosis, and bilateral laminar pleural effusions were also noted, with no evidence of a primary neoplasm or metastatic disease. Atrial fibrillation was documented on electrocardiography, and the internal medicine team interpreted the findings as left atrial thrombus with visceral embolism. Anticoagulation with unfractionated heparin was initiated, and transthoracic echocardiography was requested.

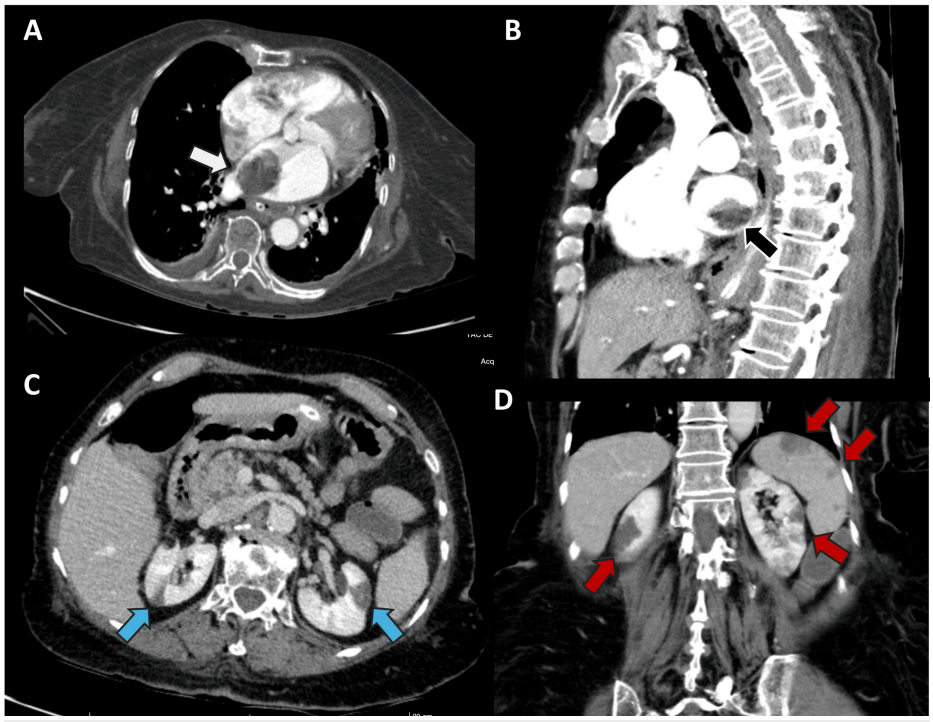


FIGURE 1: Contrast-enhanced CT of the chest (arterial phase) and abdomen (portal venous phase)

CT: computed tomography

(A) Axial image at the level of the heart showing an oval, lobulated intraluminal mass in the left atrium (white arrow). (B) Sagittal reconstruction showing the intracavitary left atrial mass with heterogeneous enhancement (black arrow). (C) Axial abdominal image showing wedge-shaped hypodense areas in the renal parenchyma, consistent with established infarcts (blue arrows). (D) Coronal abdominal reconstruction showing the multifocal distribution of bilateral splenic and renal infarcts (red arrows)

Before echocardiography could be performed, the patient developed sudden left hemiparesis, mild dysarthria, and left facial palsy. CT angiography of the brain showed no large-vessel occlusion (Alberta Stroke Program Early CT Score of 10). Brain MRI demonstrated multiple acute lesions with restricted diffusion and corresponding T2 and fluid-attenuated inversion recovery (FLAIR) hyperintensity, in cortical

and subcortical locations of both frontoparietal regions, predominantly on the right and involving the right precentral and postcentral gyri, as well as in the right occipital and periatrial regions (Figure 2). No hemorrhagic changes were identified on any sequence. Involvement of noncontiguous territories supported an embolic mechanism and raised suspicion of a proximal cardiac source [7,12]. Intravenous thrombolysis was withheld because of active gastrointestinal bleeding and ongoing anticoagulation with unfractionated heparin, and mechanical thrombectomy was not indicated because no large-vessel occlusion was identified [13].

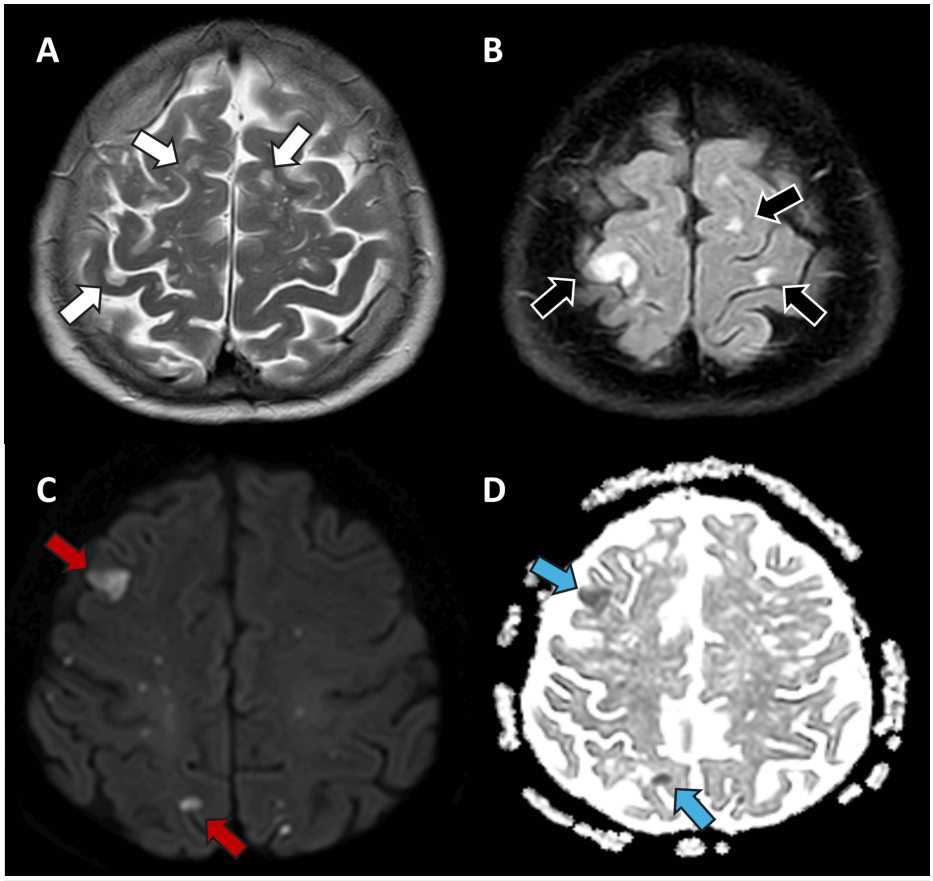


FIGURE 2: Brain MRI

MRI: magnetic resonance imaging; FLAIR: fluid-attenuated inversion recovery

(A) Axial T2-weighted image showing cortical and subcortical hyperintense areas (white arrows). (B) Axial FLAIR image showing the same lesions with better delineation from cerebrospinal fluid (black arrows). (C) Axial diffusion-weighted image showing restricted diffusion in multiple cortical and subcortical foci (red arrows). (D) Apparent diffusion coefficient map at the same level showing hypointensity in the corresponding areas (blue arrows), consistent with acute infarcts in a distribution suggestive of cardioembolism

Transthoracic echocardiography revealed a mobile, heterogeneous 50 × 32 mm mass in the left atrium, apparently attached to the interatrial septum with areas of contact with the lateral wall; myxoma was the leading diagnostic consideration, with organized thrombus as the differential (Figure 3). Transesophageal echocardiography was not performed. Almost simultaneously, the patient lost bilateral pulses from the popliteal level distally, with cold extremities, sensory deficit, and painful compartments. CT angiography of the lower limbs showed filling defects consistent with acute embolic occlusion of the P2-P3 popliteal segments and of the tibioperoneal trunks bilaterally, classified as Rutherford IIA on the right and IIB on the left. The abdominal acquisition showed segmental hypodensity with absent mucosal enhancement of the cecum and distal ileum, without pneumatosis, pneumoperitoneum, or free fluid, consistent with segmental ischemia in the ileocolic territory, together with the previously identified renal and splenic infarcts (Figure 4). The ileocolic artery occlusion was not directly visualized and was inferred from these bowel findings. Combined emergency surgery was scheduled.

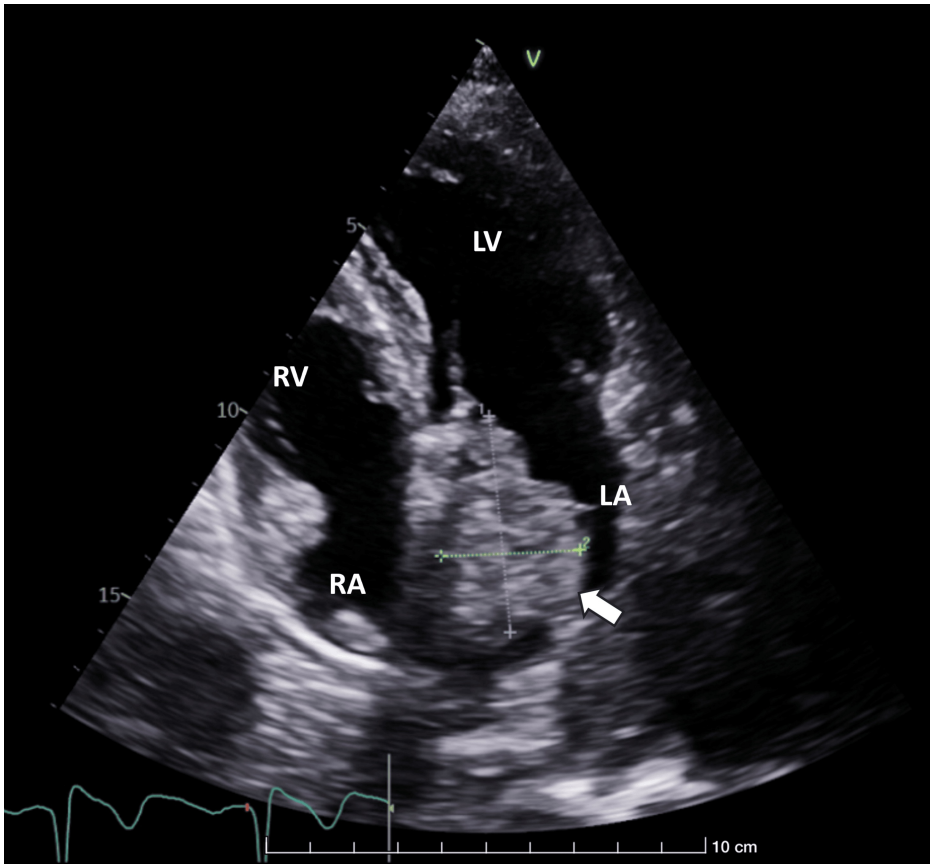


FIGURE 3: Transthoracic echocardiogram, apical four-chamber view

LA: left atrium; LV: left ventricle; RA: right atrium; RV: right ventricle

Mobile, heterogeneous left atrial mass measuring 50 × 32 mm with poorly defined margins (arrow), apparently attached to the interatrial septum with areas of contact with the lateral wall; at surgery, the pedicle was located on the inferior atrial wall below the ostia of the right pulmonary veins. Myxoma was the leading diagnostic consideration



FIGURE 4: Contrast-enhanced CT angiography

CT: computed tomography

(A) Axial images and (B) coronal reconstruction showing intraluminal filling defects in the P2-P3 segments of both popliteal arteries (white arrows), consistent with acute embolic occlusion. (C) Axial image and (D) coronal abdominal reconstruction showing segmental hypodensity of the cecum with absent mucosal enhancement (black arrows), consistent with segmental ischemia in the ileocolic territory

Exploratory laparotomy revealed a moderate amount of turbid peritoneal fluid, dilated and hypoperfused small bowel loops without frank necrosis, and transmural necrosis of the cecum and ileocecal valve with thrombosed ileocolic vessels. A partial right colectomy with distal ileostomy was performed; the abdomen was left open under negative pressure therapy; and the stapled bowel ends were left in place for a planned second-look procedure. Bilateral lower limb embolectomy was performed immediately afterward. The retrieved material was yellowish, friable, and gelatinous, unlike conventional organized thrombus, and histopathologic examination confirmed myxomatous tissue. Distal pulses were restored in both extremities.

The following day, the patient underwent median sternotomy with cardiopulmonary bypass and del Nido cardioplegia for resection of the left atrial mass. Intraoperatively, the tumor had a morular, gelatinous, and hemorrhagic gross appearance, and its pedicle was located on the inferior atrial wall below the ostia of the right pulmonary veins. Complete excision was achieved, with curettage of the implantation site and irrigation of the cardiac chambers. Histopathologic examination confirmed cardiac myxoma, with spindle and stellate cells embedded in a loose, mucopolysaccharide-rich myxoid matrix, neovascularization, and hemorrhagic foci; immunohistochemistry was positive for calretinin and CD31 (Figure *5*) [1,4]. After cardiac manipulation, the right leg sustained a new embolic event requiring reintervention with segmental popliteal resection and end-to-end anastomosis.

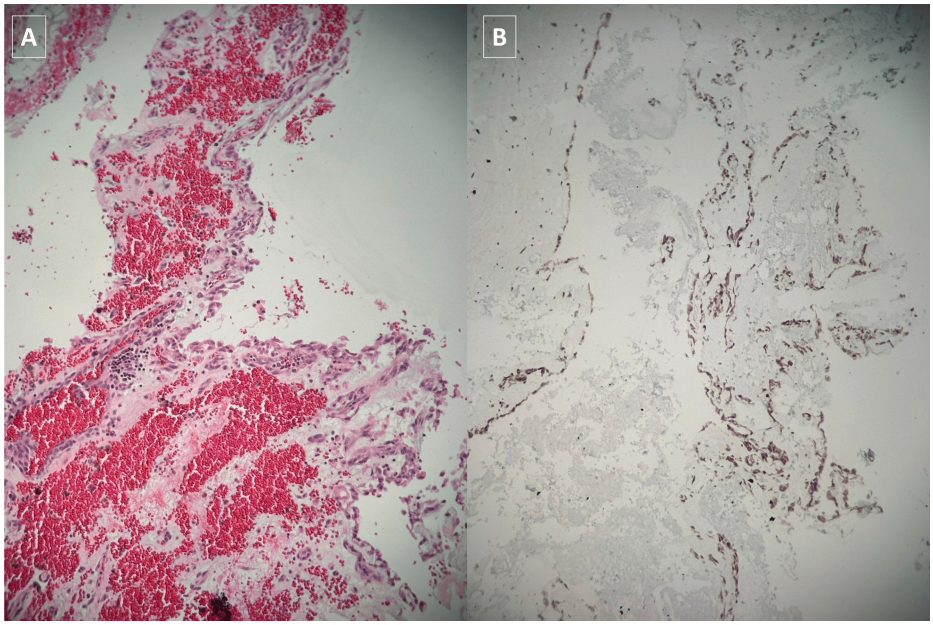


FIGURE 5: Histopathologic examination of the resected atrial mass

(A) Hematoxylin and eosin staining (200×) showing a loose myxoid stroma with spindle and stellate cells (myxoma cells) surrounded by abundant hemorrhagic material; no atypical mitotic activity or tumor necrosis is identified. (B) Immunohistochemistry using the polymer-peroxidase technique (200×) showing positivity for calretinin, the marker most supportive of cardiac myxoma, and for CD31 in scattered tumor cells within the myxoid stroma. The diagnosis rests on the combined morphologic and immunohistochemical findings

Several days later, follow-up abdominal CT revealed new extensive small bowel ischemia involving the jejunum and ileum, peritonitis, and free intraperitoneal air. Whether this represented new embolization or progression of the prior mesenteric ischemia could not be determined. The patient deteriorated hemodynamically and underwent emergency laparotomy, which confirmed four-quadrant fecal peritonitis secondary to anastomotic dehiscence; a damage-control approach was used. Despite maximal intensive care support with dual vasopressor therapy, she developed progressive oliguria and multiorgan hypoperfusion and died two weeks after admission.

Discussion

Multiterritorial embolization from left atrial myxoma has been described previously [8,14]. The contribution of this report is therefore educational rather than a claim of rarity: it illustrates how a left atrial mass initially read as thrombus on CT can be reassessed when infarcts accumulate in several vascular beds, in an 86-year-old patient whose clinical context strongly favored thrombus.

The initial interpretation of thrombus was reasonable. The patient was elderly, had electrocardiographically documented atrial fibrillation and left atrial enlargement, and already showed visceral infarcts, all of which point toward thromboembolic disease. In retrospect, however, several CT features favored myxoma. On retrospective review by a radiologist with expertise in thoracic imaging, the mass was oval with lobulated contours, showed unequivocal heterogeneous enhancement, and was related to the interatrial septum rather than to the left atrial appendage, the most frequent site of thrombus. Its size (45 mm) also exceeded that typical of left atrial thrombi; in the comparative CT series of Scheffel et al., myxomas were significantly larger than thrombi (mean, 33 vs. 21 mm), and size, site of origin, shape, mobility, and prolapse, rather than attenuation, distinguished the two entities [9]. The same authors noted that first-pass arterial acquisitions may be too early to show tumor enhancement [9], which makes the enhancement visible in our patient on an arterial-phase study a relevant clue. Grebenc et al. described most myxomas on CT as lobulated, hypoattenuating, and heterogeneous masses [11], and myxomas may enhance heterogeneously whereas thrombi are typically avascular [10]. These features modify the probability of myxoma but do not establish the diagnosis, since organized thrombi can be heterogeneous and occasionally show peripheral enhancement [10].

Both CT and transthoracic echocardiography suggested attachment to the interatrial septum, whereas surgery located the pedicle on the inferior atrial wall below the ostia of the right pulmonary veins, a region close to the posterior aspect of the septum. A large, lobulated, mobile mass in broad contact with the septum can obscure the true pedicle on both modalities; Scheffel et al. likewise reported CT misclassification of myxoma origin in two of 13 cases [9]. Transesophageal echocardiography, which was not performed, might have defined the attachment more precisely. A nonfossa ovalis origin is also relevant

because atypical tumor location is a reported risk factor for embolization [5].

Multimodality imaging defined the embolic burden. The initial CT documented established renal and splenic infarcts; brain MRI showed acute infarcts in noncontiguous cortical and subcortical territories of both hemispheres, a distribution suggestive of cardioembolism but not specific for myxoma [7,12]; and CT angiography demonstrated bilateral popliteal and tibioperoneal occlusions and bowel findings of ischemia in the ileocolic territory, with thrombosis of the ileocolic vessels confirmed at surgery. In total, five vascular beds were involved: the cerebral, renal, splenic, ileocolic mesenteric, and lower-limb arteries. Although the patient had diffused calcified atherosclerosis, the abrupt bilateral onset, the involvement of multiple noncontiguous beds, and the histology of the retrieved material support an embolic rather than in situ thrombotic mechanism. The risk profile was consistent with published data: in a meta-analysis of 1,814 patients, Liu et al. identified hypertension, irregular tumor surface, atypical location, a narrow attachment base, and elevated fibrinogen as risk factors for embolization [5], and Amemiya et al. found villous external morphology to be the strongest independent predictor of embolic events, with an odds ratio of 8.7 [6]. The morular, gelatinous, and friable appearance of our patient's tumor is compatible with, but not diagnostic of, this villous subtype [6,14].

The practical lesson is that, when an intracardiac mass coexists with systemic infarcts, prompt echocardiographic characterization and direct communication between radiologists and the treating team may shorten the interval to diagnosis. In our patient, the cerebral and lower-limb events occurred before echocardiography was performed; whether earlier recognition would have changed the outcome cannot be determined. Cardiac MRI was not performed because of the patient's instability; had it been feasible, heterogeneous late gadolinium enhancement would have favored myxoma, whereas thrombi remain avascular and hypointense on long-inversion-time images [10,15].

Surgical priorities were set by the immediate threats to limb and bowel viability. Bowel necrosis and bilateral Rutherford IIA/IIB ischemia required intervention within hours, whereas cardiac surgery with cardiopulmonary bypass in an 86-year-old patient with active ischemic injury carried substantial risk; the trade-off was the competing risk of further embolization from the unresected mass, which was excised the following day. This sequence reflects the decision in this specific context and should not be generalized as a treatment algorithm. Settembrini et al. noted that the gross appearance of retrieved emboli should raise suspicion of a myxomatous origin and prompt cardiac evaluation, and reported an in-hospital mortality of 12.1% in 59 patients presenting with acute limb ischemia due to myxoma embolization [14].

Advanced age adds risk to every step of management, and elderly patients may not be ideal candidates for cardiac surgery [1]. Reported mortality after myxoma excision ranges from 3.75% in a single-center series of 80 patients [2] to 10% in another series, with 0% to 10% 30-day mortality reported in the literature [3]. Patients with acute thromboembolic ischemia and those older than 80 years were excluded from the former series [2], so data for patients like ours are scarce. The immediate cause of death in our patient was septic shock from anastomotic dehiscence and fecal peritonitis, a postoperative complication that should be distinguished from the earlier consequences of embolization and should not be interpreted as failure of tumor resection.

This report has several limitations. First, as a single case, it cannot establish the diagnostic performance of any CT feature or the generalizability of the management sequence. Second, the retrospective CT review was performed after histopathologic confirmation and may be influenced by knowledge of the final diagnosis, whereas the original interpretation was made without it. Third, quantitative attenuation measurements of the mass were not available, so enhancement was assessed qualitatively. Fourth, neither transesophageal echocardiography nor cardiac MRI was performed, which limited assessment of the tumor attachment. Finally, the complex clinical course, the multiple surgical interventions, and the extensive pre-existing ischemic injury make it impossible to isolate the contribution of any single diagnostic or therapeutic decision to the outcome, including the mechanism of the late small bowel ischemia.

Conclusions

A left atrial filling defect accompanied by infarcts in multiple vascular beds should prompt early echocardiographic characterization and consideration of myxoma, even when the clinical context favors thrombus. Large size, lobulated contours, heterogeneous enhancement, and a location outside the left atrial appendage are CT features that increase the likelihood of myxoma, although none is definitive. Careful assessment of the mass, recognition of the embolic distribution, and timely communication between radiologists and the treating team may help reduce diagnostic delay, while the definitive diagnosis remains histopathologic.

Additional Information

Author Contributions

All authors have reviewed the final version to be published and agreed to be accountable for all aspects of the work.

Concept and design: Sergio Rueda Góez, Tatiana Suárez Poveda

Acquisition, analysis, or interpretation of data: Sergio Rueda Góez, Mateo Zapata Naranjo, Tatiana Suárez Poveda, Miguel Roldán Pérez

Drafting of the manuscript: Sergio Rueda Góez, Mateo Zapata Naranjo, Tatiana Suárez Poveda, Miguel Roldán Pérez

Critical review of the manuscript for important intellectual content: Sergio Rueda Góez, Tatiana Suárez Poveda

Disclosures

Human subjects: Informed consent for treatment and open access publication was obtained or waived by all participants in this study. **Conflicts of interest:** In compliance with the ICMJE uniform disclosure form, all authors declare the following: **Payment/services info:** All authors have declared that no financial support was received from any organization for the submitted work. **Financial relationships:** All authors have declared that they have no financial relationships at present or within the previous three years with any organizations that might have an interest in the submitted work. **Other relationships:** All authors have declared that there are no other relationships or activities that could appear to have influenced the submitted work.

References

1. Okongwu CC, Olaofe OO: Cardiac myxoma: a comprehensive review. J Cardiothorac Surg. 2025, 20:151. 10.1186/s13019-024-03333-2
2. Alhasso AA, Ahmed OF, Mohammed-Saeed DH, et al.: Operative management and outcomes in patients with myxomas: a single-center experience. Front Surg. 2023, 10:1084447. 10.3389/fsurg.2023.1084447
3. Hadiya N, Kumar M, Parshad R, Chandar P, Gupta A: Clinical characteristics and surgical outcomes following cardiac myxoma resection. J Cardiovasc Thorac Res. 2025, 17:35-9. 10.34172/jcvtr.025.33237
4. Velez Torres JM, Martinez Duarte E, Diaz-Perez JA, Rosenberg AE: Cardiac myxoma: review and update of contemporary immunohistochemical markers and molecular pathology. Adv Anat Pathol. 2020, 27:380-4. 10.1097/PAP.0000000000000275
5. Liu Y, Wang J, Guo L, Ping L: Risk factors of embolism for the cardiac myxoma patients: a systematic review and metanalysis. BMC Cardiovasc Disord. 2020, 20:348. 10.1186/s12872-020-01631-w
6. Amemiya K, Yonemoto Y, Ishibashi-Ueda H, et al.: Morphological characteristics of cardiac myxoma causing embolism: a series of 40 years of experience at a single institute. Virchows Arch. 2023, 482:377-84. 10.1007/s00428-022-03461-x
7. Pérez Andreu J, Parrilla G, Arribas JM, et al.: Neurological manifestations of cardiac myxoma: experience in a referral hospital. Neurologia. 2013, 28:529-34. 10.1016/j.nrl.2013.03.006
8. Manresa-Manresa F, Aragón-Ropero PP, Canalejo-Raya MA, et al.: Multiple embolism from giant left atrial myxoma in a young patient (Article in Spanish). Cardiocore. 2017, 52:129-31. 10.1016/j.carcor.2016.03.005
9. Scheffel H, Baumueller S, Stolzmann P, Leschka S, Plass A, Alkadhi H, Schertler T: Atrial myxomas and thrombi: comparison of imaging features on CT. AJR Am J Roentgenol. 2009, 192:639-45. 10.2214/AJR.08.1694
10. Hrabak-Paar M, Muršić M, Balaško-Josipović T, Dilber D, Bulj N: Multimodality imaging of cardiac myxomas. Rev Cardiovasc Med. 2024, 25:204. 10.31083/j.rcm2506204
11. Grebenc ML, Rosado-de-Christenson ML, Green CE, Burke AP, Galvin JR: Cardiac myxoma: imaging features in 83 patients. Radiographics. 2002, 22:673-89. 10.1148/radiographics.22.3.g02ma02673
12. Cotrim N, Veiga AR, Castilho B, Peres M, Martins V: Giant cardiac myxoma as a cause of stroke . JACC Case Rep. 2024, 29:102866. 10.1016/j.jaccas.2024.102866
13. Powers WJ, Rabinstein AA, Ackerson T, et al.: Guidelines for the early management of patients with acute ischemic stroke: 2019 update to the 2018 guidelines for the early management of acute ischemic stroke: a guideline for healthcare professionals from the American Heart Association/American Stroke Association. Stroke. 2019, 50:e344-418. 10.1161/STR.0000000000000211
14. Settembrini AM, Foresti L, Verlato P, et al.: Acute lower limb ischaemia as a presenting sign of atrial myxoma: case report and scoping review of the literature. EJVES Vasc Forum. 2024, 62:35-40. 10.1016/j.ejvsvf.2024.07.036
15. Abbas A, Garfath-Cox KA, Brown IW, Shambrook JS, Peebles CR, Harden SP: Cardiac MR assessment of cardiac myxomas. Br J Radiol. 2015, 88:20140599. 10.1259/bjr.20140599